Localization of Divalent Cation-Binding Site in the Pore of a Small Conductance Ca^{2+}-Activated K^+ Channel and Its Role in Determining Current-Voltage Relationship

Heun Soh and Chul-Seung Park
Department of Life Science, Kwangju Institute of Science and Technology, Gwangju 500-712, Korea

ABSTRACT In our previous study, we proposed that the inwardly rectifying current-voltage (I-V) relationship of small-conductance Ca^{2+}-activated K^+ channels (SK_{Ca} channels) is the result of voltage-dependent blockade of K^+ currents by intracellular divalent cations. We expressed a cloned SK_{Ca} channel, rSK2, in *Xenopus* oocytes and further characterized the nature of the divalent cation-binding site by electrophysiological means. Using site-directed substitution of hydrophilic residues in K^+-conducting pathway and subsequent functional analysis of mutations, we identified an amino acid residue, Ser-359, in the pore-forming region of rSK2 critical for the strong rectification of the I-V relationship. This residue interacts directly with intracellular divalent cations and determines the ionic selectivity. Therefore, we confirmed our proposition by localizing the divalent cation-binding site within the conduction pathway of the SK_{Ca} channel. Because the Ser residue unique for the subfamily of SK_{Ca} channels is likely to locate closely to the selectivity filter of the channels, it may also contribute to other permeation characteristics of SK_{Ca} channels.

INTRODUCTION

Small conductance calcium-activated potassium channels (or SK_{Ca} channels) are potassium selective, voltage-independent, and activated by an increase in the level of intracellular calcium concentration. These channels play important roles in excitable cells such as neurons in the central nervous system (Vergara et al., 1998). The activity of SK_{Ca} channels underlies the slow after-hyperpolarization that inhibits neuronal cell firing (Hille, 1991; Vergara et al., 1998). Three different but homologous complementary DNAs (cDNAs) were cloned to encode SK_{Ca} channels in higher mammals (Kohler et al., 1996). Each subtype of SK_{Ca} channels, ~550 to 730 amino acids in length, contains six putative transmembrane regions, S1 to S6, and the cytosolic amino and carboxyl termini. A pore-forming region (P-region) including the "potassium channel signature sequence (Gly-Tyr-Gly)" is found in between S5 and S6. A series of functional and structural studies showed that SK_{Ca} channels bind an auxiliary subunit, calmodulin, as the Ca^{2+}-sensing gating machinery (Xia et al., 1998; Keen et al. 1999). Because the channels are thought to exist as tetramers, four main subunits of identical or different subtypes and four calmodulins constitutively bound to carboxyl termini are assembled to form the functional SK_{Ca} channels. The opening of the channels is now understood as the result of the binding of cytosolic Ca^{2+} to calmodulin and subsequent conformational change.

Although the activation of SK_{Ca} channels is relatively insensitive to transmembrane voltage, the current-voltage (I-V) relationship of the channels is rectified inwardly in the presence of physiological concentration of divalent cations. In a recent report, we showed that intracellular divalent cations such as Ca^{2+} and Mg^{2+} specifically blocked the K^+-conducting region of SK2 channel in a voltage-dependent manner and that the voltage-dependent blockade by intracellular divalent cations underlies the inward rectification of SK_{Ca} channel (Soh and Park, 2001). The mechanism of the inwardly rectifying I-V relationship revealed for SK_{Ca} channel is reminiscent of the inward-rectifier K^+ channels (or K_{ir} channels) whose I-V relationship is also rectified inwardly due to the blockade of channel currents by intracellular cations such as Mg^{2+} and polyamines (Matsuda et al., 1987; Vandenberg, 1987; Lopatin and Nichols, 1996). A hydrophilic amino acid residue within the second transmembrane region (M2) was identified as the binding site for intracellular Mg^{2+} and polyamines in K_{ir} channels (Lu and MacKinnon, 1994; Wible et al., 1994). It is also known that the degree of I-V rectification is determined by the nature of the amino acid residue and that the electrostatic forces are involved in the interaction between the residue and intracellular cations (Lu and MacKinnon, 1994). The strongly rectified K_{ir} channels such as K_{ir} 2.1 and K_{ir} 4.1 have acidic residues, aspartate (Asp) or glutamate (Glu) at this position (Kubo et al., 1993; Bond et al., 1994), whereas the weak inward rectifiers such as K_{ir}1.1 and K_{ir} 5.1 contain neutral but hydrophilic residues, asparagines (Asn) (Ho et al., 1993; Bond et al., 1994; see Fig. 2 *A*).

In this study, we searched for the amino acid residues of the K^+-conducting pathway interacting with intracellular divalent cations and affecting the I-V relationship of a SK_{Ca} channel, rSK2. We replaced several hydrophilic residues predicted to be in the channel pore to alanine (Ala), and investigated the effects of mutations on both I-V relationships and the affinity of intracellular divalent cations using

Submitted October 10, 2001; and accepted for publication June 27, 2002.
Address reprint requests to Chul-Seung Park, PhD, Department of Life Science, Kwangju Institute of Science and Technology (*K-JIST*), 1 O-ryong-dong, Buk-gu, Gwangju 500-712, Korea. Tel.: 82-62-970-2489; Fax: 82-62-970-2484; E-mail: cspark@kjist.ac.kr.
© 2002 by the Biophysical Society
0006-3495/02/11/2528/11 $2.00

electrophysiological methods. We found that a serine residue, Ser-359, within the P-region interacts directly with divalent cations and affects the degree of I-V rectification. Based on the known structure of the KcsA K^+ channel (Doyle et al., 1998), the binding site revealed in this study for SK_{Ca} channels is likely to be near the K^+-selectivity filter, which is markedly different from the Mg^{2+}-binding site of K_{ir} channels predicted to be in the "central cavity." Therefore, we confirmed that the inwardly rectifying I-V relationship of SK_{Ca} channels is due to the blockade of K^+ currents by intracellular divalent cations by localizing the binding site and showed that the mechanistic similarity of I-V rectification for SK_{Ca} and K_{ir} channels bifurcate clearly at the molecular level.

MATERIALS AND METHODS

Expression of rSK2 channels in *Xenopus* oocytes

All electrophysiological experiments were done on wild-type or mutant rSK2 channels expressed in *Xenopus* oocytes. *Xenopus* laevis (*Xenopus*-One, Dexter, MI) was cared for and handled as described previously in accordance with the highest standards of institutional guidelines (Soh and Park, 2001). The complementary DNA for rSK2 channels was provided by Dr. J.P. Adelman (The Vollum Institute, Oregon Health Sciences University, Portland, OR) and subcloned into modified pGH expression vector for high-level expression in *Xenopus* oocytes. Complementary RNAs for rSK2 channels were synthesized in vitro from a *Nco*I-linearized plasmid using T7 polymerase (Promega, Medison, WI). Oocytes were injected with approximately 50 ng of RNA, and the injected oocytes were incubated at 18°C for 3 to 7 days in ND96 solution containing 5 mM HEPES, 96 mM NaCl, 2 mM KCl, 1.8 mM $CaCl_2$, 1 mM $MgCl_2$, and 50 μg/mL gentamicin, pH 7.6, adjusted with NaOH.

Construction of mutant rSK2 channels

Silent mutations of rSK2 were introduced in amino acid positions 288, 395, and 396 (sequence numbering according to Kohler et al., 1996) to produce *Bgl*II (from AGAAGC to AGATCT) and *Bss*HII (from GCAAGG to GCGCGC) restriction sites using two sequential polymerase chain reactions, respectively. Cassette mutagenesis was performed to replace specific amino acid residues within the P-region and S6 of rSK2. Mutations were generated by polymerase chain reaction using mutagenic primers, and the amplified DNA fragments flanked by *Bgl*II and *Bss*HII were replaced for wild-type gene. DNA sequence of each mutant channel was confirmed by subsequent sequencing analysis.

Electrophysiological recordings

Ionic currents carried by wild-type and mutant rSK2 channels were recorded from patches of oocyte membrane in inside-out configuration using an Axopatch 200B amplifier (Axon Instruments, Foster City, CA). Patch recordings were performed at room temperature (23°C) 3 to 7 days after RNA injection. Pipettes prepared from thin-walled borosilicate glass (World Precision Instruments, Sarasota, FL) had resistance of 1 to 4 MΩ. Signals were filtered at 1 kHz using a four-pole low-pass Bessel filter, digitized at a rate of 200 samples/ms using Digidata 1200 (Axon Instruments) and stored in a personal computer. pClamp8 software (Axon Instruments) was used to control the amplifier and to acquire the data. For macroscopic current recordings, the membrane was held at 0 mV and ramped from -100 to 100 mV over 1 s. To ensure that a steady-state blockade was achieved throughout the ramp, the current blockade by internal divalent was determined using an independent protocol of voltage steps lasting 100 ms. These control experiments gave the same results and therefore validated the use of ramps to accurately measure the current blockade. We observed a variable degree of channel rundown in the absence of any treatment in ~30% of patches. Patches exhibiting severe rundown, in that channel activity was lost within the first minute of recording, were excluded from the analysis.

Pipette (or extracellular) solutions contained 10 mM HEPES (Gibco BRL, Rockville, MD), 2 mM EGTA, 116 mM KOH, and 4 mM KCl. Excised patches were perfused with an intracellular solution containing 10 mM HEPES, 2 mM EGTA, 116 mM KOH, and 4 mM KCl, supplemented with $CaCl_2$. For Mg^{2+}, Sr^{2+}, or Ba^{2+} blocking experiments, $MgCl_2$, $SrCl_2$, or $BaCl_2$ was added to give desired free concentration. The amount of $MgCl_2$, $CaCl_2$, $SrCl_2$, or $BaCl_2$ required to yield the concentration indicated was calculated according to the following stability constants (log K): Mg-EGTA, 5.28; Ca-EGTA, 10.86; Sr-EGTA, 8.43; and Ba-EGTA, 8.3 (Martell and Smith, 1974). The pH of all recording solutions was adjusted to 7.2 with methanesulfonate. The calculation included an adjustment for pH. To activate channel currents for blocking experiments of Mg^{2+}, Sr^{2+}, or Ba^{2+}, 2 μM of Ca^{2+} was added into the intracellular solution. Activation and blockade were measured by perfusing the intracellular face of the membrane patch with solutions containing different concentrations of divalent cations. All compounds for the recording solution were obtained from Sigma/Aldrich Chemical (St. Louis, MO) unless otherwise specified.

RESULTS

Ionic currents of rSK2 channel are blocked by divalent cations, Mg^{2+}, Ca^{2+}, Sr^{2+}, and Ba^{2+}

In our recent study, we showed that rSK2 channels are blocked by internal Mg^{2+} and Ca^{2+} in a voltage-dependent manner causing the inwardly rectified I-V relationship and proposed that the binding site of the divalent cations is within the channel conduction pore (Soh and Park, 2001). We first examined the effects of other alkaline earth metals on the blocking of the rSK2 channel currents. Fig. 1 *A* shows the representative macroscopic currents blocked by three different divalent cations, Mg^{2+}, Sr^{2+}, and Ba^{2+}, in the presence of 2 μM intracellular calcium concentration, $[Ca^{2+}]_i$. In the case of Ca^{2+}, both of the activation occurring at submicromolar range and the blockade happening at tens to hundreds of micromolar ranges were measured at increasing concentration of $[Ca^{2+}]_i$. Although all four divalent cations block the rSK2 channel currents and render strong inward rectifications to the I-V relationships, the effective concentration ranges are markedly different among these divalent cations. Although Ba^{2+} blocks rSK2 channel currents with the highest affinity ($^{Ba}K_i = 0.6$ μM), Mg^{2+} can achieve a similar level of current reduction at a concentration range of approximately three-orders of magnitude higher. In Fig. 1 *B*, the current blockade was measured at 90 mV and plotted against various concentrations of each divalent cation tested. Data points are fitted to the Hill equation, and the inhibition constants (K_i) for Mg^{2+}, Ca^{2+}, Sr^{2+}, and Ba^{2+} were determined (Table 1). The binding site within the K^+-conduction pore of the rSK2 channel exhibits a strong size-selectivity for larger divalent

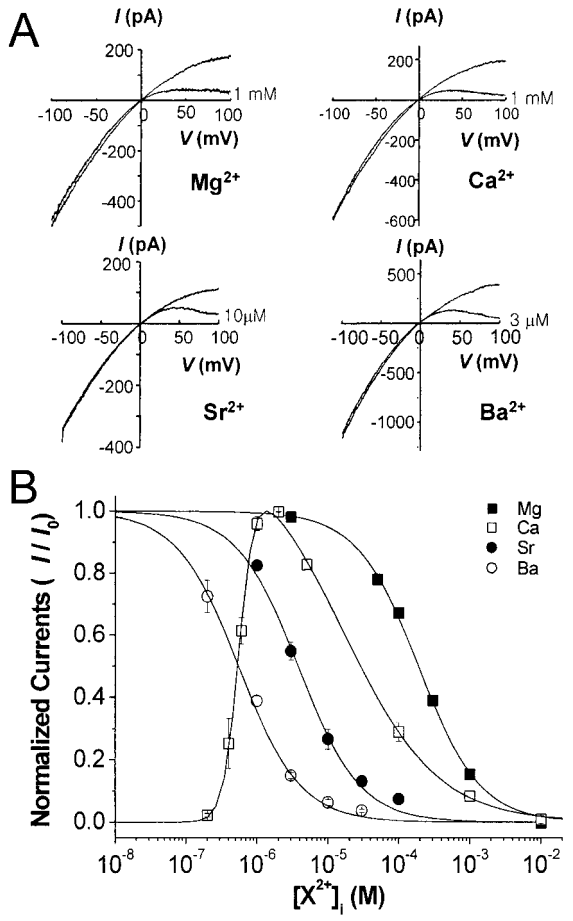

FIGURE 1 Blockade of rSK2 channel currents by alkali earth metals. (*A*) Representative traces of rSK2 control currents activated by 2 μM intracellular Ca^{2+} and the current trace in the presence of indicated concentration of intracellular divalent cation in addition to Ca^{2+} were shown for four different divalent cations, Mg^{2+}, Ca^{2+}, Sr^{2+}, and Ba^{2+}. (*B*) Fraction of unblocked currents (I/I_o) obtained from the normalized currents at 90 mV were plotted against different concentration of each divalent divalent cation, $[X^{2+}]_i$. The lines superimposed on the data points correspond to least-squares fits using the Hill equation. In the case of Ca^{2+} blockade, since Ca^{2+} also activate the rSK2 channels in the submicromolar range, data points are fitted to $y = V_{max}*(x^n/(K_{1/2}{}^n + x^n))*(x^{-m}/({}^{Ca}K_i{}^{-m} + x^{-m}))$; y, fraction of unblocked currents; x, concentration of intracellular Ca^{2+}; $K_{1/2}$, the activation constant; ${}^{Ca}K_i$, inhibition constant; n, Hill coefficient for activation; $-m$, Hill coefficient for blockade. The observed inhibition constants of each divalent cation were shown in Table 1.

cations, $Mg^{2+} < Ca^{2+} < Sr^{2+} < Ba^{2+}$, and the selectivity follows a sequence of a "weak-field strength" site for divalent cations (Hille, 1991).

Comparison of SK_{Ca} and K_{ir} channels: localization of amino acid residues affecting the I-V rectification

Two lines of evidence suggested that the mode of current blockade by intracellular divalent cations and thus the molecular mechanism of inwardly rectified I-V relationship of SK_{Ca} channels might be similar to that of K_{ir} channels (Soh and Park, 2001). First, inward rectification is produced by the voltage-dependent blockade of intracellular Mg^{2+}. Second, high concentrations of extracellular K^+ reduce the affinity as well as the voltage-dependence of Mg^{2+} blockade. In the case of K_{ir} channels, a strong inward rectification is achieved by the electrostatic interaction between the intracellular Mg^{2+} (or polyamines) with a negatively charged residue in the M2 region (Lu and MacKinnon, 1994). Neutralization of this residue weakens the interaction and thus causes the shape of the I-V relationship of the channel to be less rectified. The mechanistic similarity for inward rectification between K_{ir} and SK_{Ca} channels prompted us to compare the primary amino acid sequence between the M2 region of K_{ir} channels and the corresponding S6 region of SK_{Ca} channels. Fig. 2 *A* shows the membrane topology and the amino acid sequence alignment between the members of the SK_{Ca} and K_{ir} channel families. Two hydrophilic residues, Thr-379 and Thr-387, are found within the predicted S6 region of rSK2 channels and the latter residue is aligned with the residues determining the shape of the I-V relationship in K_{ir} channels, e.g., Asp-172 in $K_{ir}2.1$. To examine whether the hydrophilic residues within the S6 region are responsible for the intracellular cation blockade of SK_{Ca} channels, both Thr residues (Thr-379 and Thr-387) and the adjacent Cys residue (Cys-386) of rSK2 were mutagenized individually to Ala, and the effects were investigated. The mutant channels were robustly expressed in *Xenopus* oocytes (data not shown), and the Ca^{2+}-depedent activation of these channels were virtually identical with that of the wild-type channel (Fig. 3 *B*). The mutations in the S6 region, however, did not alter the shape of the I-V rectification notably (Fig. 4 *A*). The I-V curves of

TABLE 1 Summary of inhibition constants (K_i) and the differences in free energy of binding ($\Delta\Delta G$) of each divalent cation for rSK2 wild-type and mutant channels

	Wild type	S359A	S359T	T379A	C386A	T387A	$\Delta\Delta G^{WT\square 359A}$
Mg^{2+}	180 ± 40 μM	180 ± 50 μM	270 ± 30 μM	250 ± 10 μM	190 ± 30 μM	190 ± 20 μM	0 kcal/mol
Ca^{2+}	19.3 μM	87.7 μM	301.3 μM	13.5 μM	25.3 μM	ND*	0.5 kcal/mol
Sr^{2+}	3.8 ± 0.4 μM	176.7 ± 6.2 μM	121.2 ± 11.2 μM	1.6 ± 0.1 μM	2.9 ± 0.1 μM	2.9 ± 0.3 μM	2.3 kcal/mol
Ba^{2+}	0.6 ± 0.1 μM	30.3 ± 1.3 μM	5.7 ± 0.4 μM	0.6 ± 0.1 μM	0.7 ± 0.1 μM	0.5 ± 0.1 μM	2.3 kcal/mol

ΔG values were calculated from K_i, $\Delta\Delta G = RT \ln K_i(\text{mutant})/K_i(\text{wild type})$.
ND*, The K_i value for the T387A mutation was not determined.

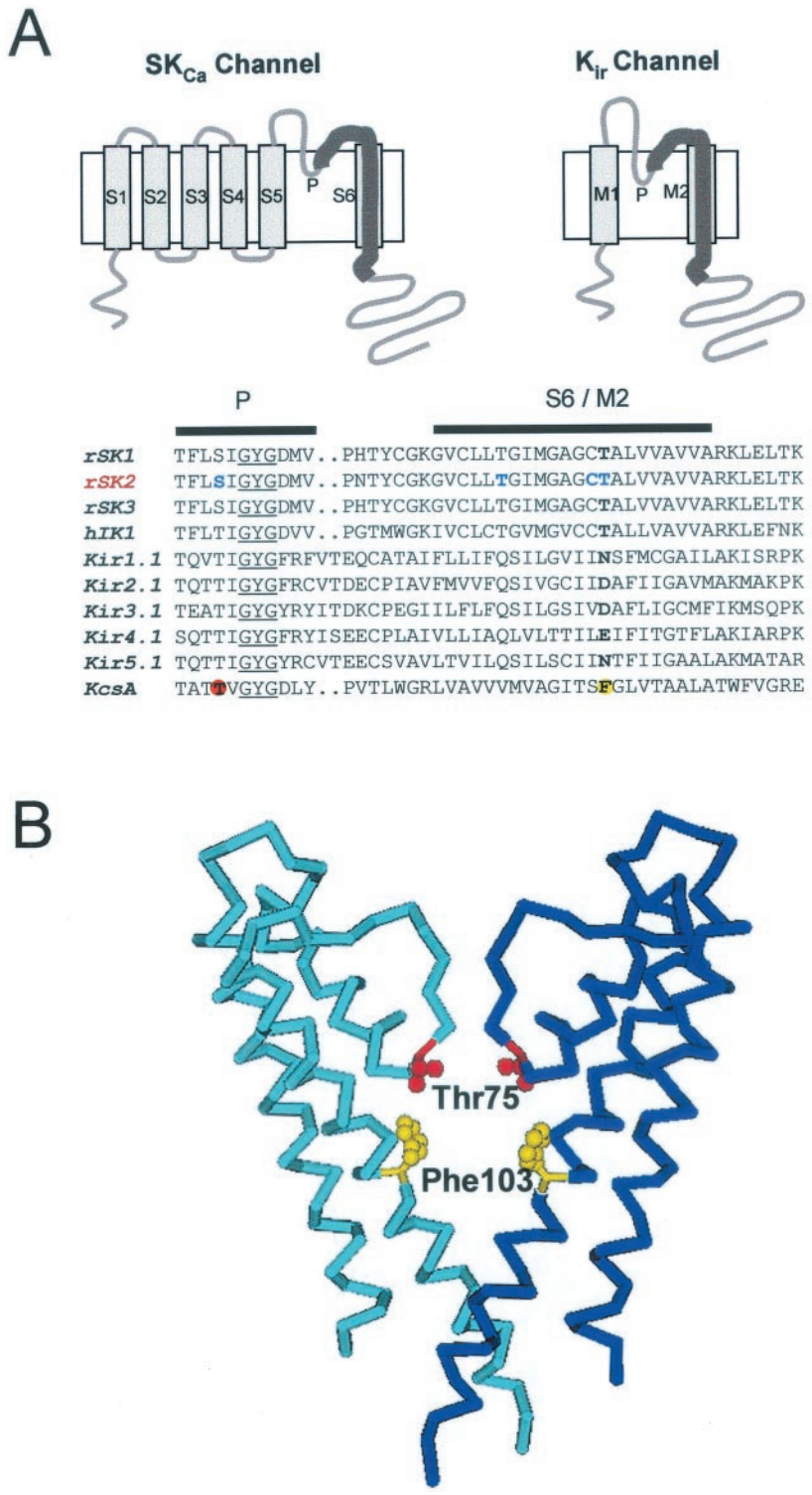

FIGURE 2 Comparison of membrane topology and amino acid sequence comprising the ion conduction pathway among K^+ channels, SK_{Ca}, K_{ir}, and KcsA channels. (*A*) The membrane topology of SK_{Ca} and K_{ir} channels was compared (*upper panel*). The protein regions spanning the C-terminal half of the P-region and the S6 or M2 are highlighted with thick lines. Amino acid sequences (in single-letter code) corresponding to the P-regions and S6 or M2 were compared for K^+ channel subfamilies of SK_{Ca}, K_{ir}, and KcsA channels (*lower panel*). Four amino acid residues, S359, T379, C386, and T387 of rSK2 mutated in this study were shown (*blue*). The amino acid residues determined to interact with intracellular cations in K_{ir} channels (Lu and MacKinnon; 1994; Wible et al., 1994) and the corresponding positions in other K^+ channels were shown (*bold*). Thr-75 (*red*) and Phe-103 (*yellow*) of the KcsA channel are aligned with Ser-359 and Thr-387 of rSK2, respectively. The K^+ signature sequences, GYG, in various K^+ channels were underlined. (*B*) The peptide backbones of two diagonally positioned KcsA K^+ channel subunits (in *light* and *dark blue*) are shown with the side chain atoms of Thr-75 and Phe-103 colored in red and yellow, respectively. The figure was prepared from the crystallographic coordinates of KcsA (PDB; 1BL8) (Doyle et al., 1998) with cn3D v.3.0 program (NCBI).

T379A (the current trace in light blue) and T387A (in black) were superimposed almost perfectly with that of wild type (in green). The relationship of C386A (in dark blue) was only slightly more linear than that of the wild-type channel. The degree of current rectification was quantified by comparing the current levels measured at 95 mV and −95 mV (Fig. 5, *A* and *B*). In the case of wild-type rSK2 channel, the magnitude of outward currents measured at 95 mV is ~35% of inward currents measured at −95 mV in the presence of 2 μM intracellular Ca^{2+}. The two mutant channels, T379A and T387A, also showed similar levels of current rectification. Although the I-V relationship of C386A display a

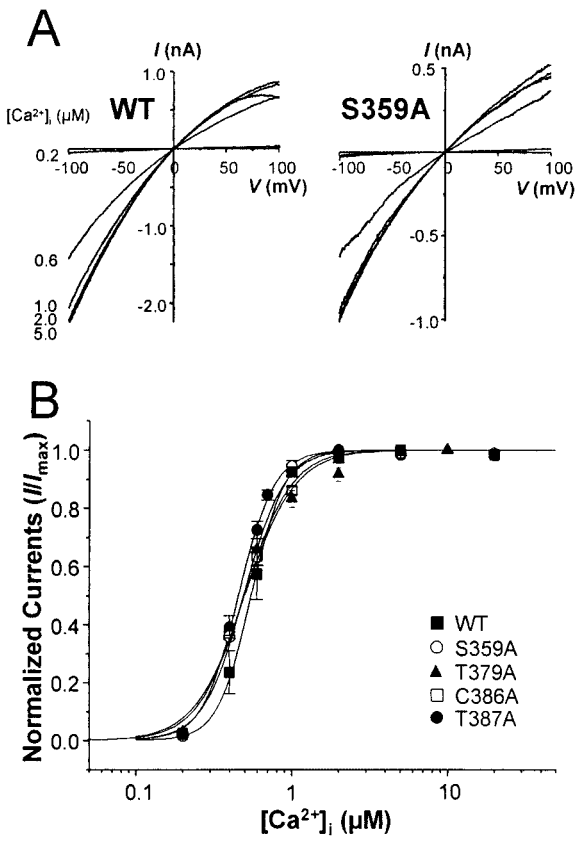

FIGURE 3 Activation characteristics of wild-type and mutant channels by intracellular Ca^{2+}. (*A*) Each current trace for wild-type and S359A mutant channels is obtained in the presence of various intracellular Ca^{2+} concentrations (0.2, 0.6, 1, 2, and 5 μM). (*B*) Fraction of activated currents obtained from the normalized current at -90 mV were plotted against $[Ca^{2+}]_i$. The lines superimposed on the data points correspond to least-squares fits using the Hill equation. The observed half-activation constants ($^{Ca}K_{1/2}$) and Hill coefficients (n) were estimated as 0.55 μM and 4.1 for wild type (■), 0.46 μM and 3.8 for S359A (○), 0.50 μM and 2.7 for T379A (▲), 0.49 μM and 3.4 for C386A (▲), and 0.50 μM and 2.9 for T387A (●).

statistically significant difference, it is only slightly less rectified than that of wild type. Thus, none of the Ala-substitution mutation at the hydrophilic residues in S6 drastically altered the I-V relationship of rSK2 channel.

In locating the amino acid residue responsible for inwardly rectifying I-V relationship, we were further guided by two lines of recent experimental results: 1) the Ba^{2+}-binding site of a bacterial K^+ channel, KcsA, was visualized by recent x-ray crystallographic study (Jiang and MacKinnon, 2000) and 2) Ba^{2+} blocks SK_{Ca} channels with high affinity and the electrical distance of the blockade, $\delta = 0.45$, is slightly larger than that of K_{ir} channels (Soh and Park, 2001). Several recent studies showed that the two transmembrane regions and the P-region of KcsA channel are analogous structurally as well as functionally to the "S5-P-region-S6" of K^+ channels containing six transmembrane regions (Shrivastava et al., 2000; Zhou et al., 2001b) and that the K^+-selective pore of the KcsA pore is likely reflective of the general structure of the K^+-conducting pathway of various K^+ channels (LeMasurier et al., 2001; Lu et al., 2001). In Fig. 2 *A*, we compared again the amino acid sequence of the P-region in SK_{Ca} channels and KcsA channel (the second and the bottom raw). We focused on the Ser-359 residue in the P-region of rSK2 (shown in blue, Fig. 2 *A*), because this residue is well aligned with Thr-75 (highlighted with red color in Fig. 2, *A* and *B*) of the KcsA channel located closely to the Ba^{2+}-binding site in the pore of KcsA channel (Jiang and MacKinnon, 2000). Therefore, we replaced this serine residue of rSK2 P-region to Ala and investigated its electrophysiological properties. The mutant channel, S359A, was expressed well in *Xenopus* oocytes (Fig. 3 *A*), and the channels currents were activated in a similar concentration range of intracellular Ca^{2+} when measured at -90 mV (Fig. 3 *B*). We noticed that the I-V relationship of S359A currents were much less rectified than that of wild type and that the negative conductance observed for wild-type channel at extreme positive voltages in the presence of greater than 5 μM $[Ca^{2+}]_i$ no longer existed for the S359A mutant channel. In Fig. 4 *A*, we compared the I-V relationships of wild type and four different mutant channels in the presence of identical concentration of intracellular Ca^{2+} at 2 μM. The I-V relationship of S359A was significantly more linear than those of wild-type and other mutant channels quantitatively (Fig. 5 *A*) as well as qualitatively (trace in red of Fig. 4 *A*). More drastic changes were observed when we added 10 μM $[Ba^{2+}]_i$ in addition to 2 μM Ca^{2+} (Figs. 4 *B* and 5 *B*). The effects of mutation on S359 were also confirmed using step protocols (Fig. 4, *C–F*). In Fig. 4, *G* and *H*, we compared the I-V relationships of the wild-type and S359A mutant channels obtained from the ramp protocol (solid lines) and the step protocol (symbols). There were no significant differences between two protocols and thus validated the instantaneous I-V relationships based on the ramp protocols. The outward currents through wild-type and all other mutant channels were blocked more than 90% at this concentration of Ba^{2+}, and their I-V relationships were rectified strongly toward the inward direction. However, the ionic currents of S359A were only slightly reduced by 10 μM $[Ba^{2+}]$, and thus, the shape of I-V relationship was only slightly affected (trace in red of Fig. 4 *B*). These results indicate that the affinities for intracellular Ca^{2+} and Ba^{2+} are much lower in the S359A mutant channel compared with wild-type or other mutant channels and strongly suggest that the Ser-359 residue is critical for the interaction with intracellular divalent cations and thus controls the degree of I-V rectification in the rSK2 channel.

Ser-359 directly interacts with intracellular divalent cations

We then examined the effects of a mutation at Ser-359 on other divalent cations in more detail. The effects of Ser to

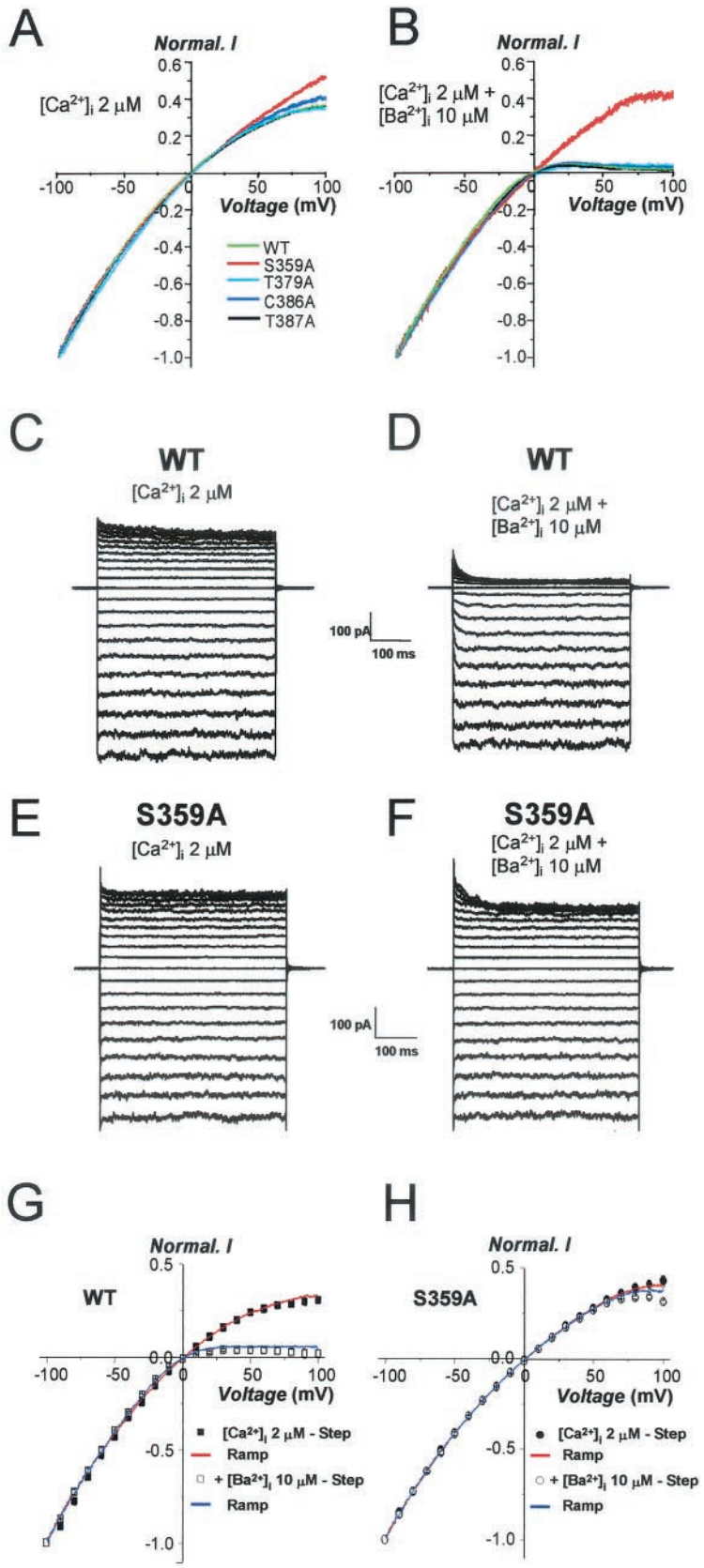

FIGURE 4 Effects of Ala-substitution on I-V relationship of rSK2 channel. (*A* and *B*) Each current trace for wild-type and mutant channels was normalized to the maximal inward current values evoked in the presence of 2 μM intracellular Ca^{2+} (*A*) and 2 μM intracellular Ca^{2+} and 10 μM Ba^{2+} (*B*), respectively. (*C* and *D*) Ionic currents elicited by a step pulse for rSK2 wild-type channel were shown in the presence of 2 μM intracellular Ca^{2+} (*C*) and 2 μM intracellular Ca^{2+} and 10 μM Ba^{2+} (*D*), respectively. The membrane was held at 0 mV and step to test voltages ranging from -100 to 100 mV in 10-mV increment for 450 ms and returned to 0 mV. (*E* and *F*) Identical protocol was applied for S359A mutant channel in the presence of 2 μM intracellular Ca^{2+} (*E*) and 2 μM intracellular Ca^{2+} and 10 μM Ba^{2+} (*F*), respectively. (*G* and *H*) Solid lines represent the normalized currents elicited by the ramp protocol in the presence of 2 μM intracellular Ca^{2+} (*red trace*) and 2 μM intracellular Ca^{2+} and 10 μM Ba^{2+} (*blue trace*) for wild-type (*G*) and S359A (*H*) channels, respectively. The symbols represent the normalized current amplitude of wild type (*rectangle*) and S359A (*circle*) after 440 ms of test pulse elicited by step pulses in the presence of 2 μM intracellular Ca^{2+} (*black symbol*) and 2 μM intracellular Ca^{2+} and 10 μM Ba^{2+} (*white symbol*).

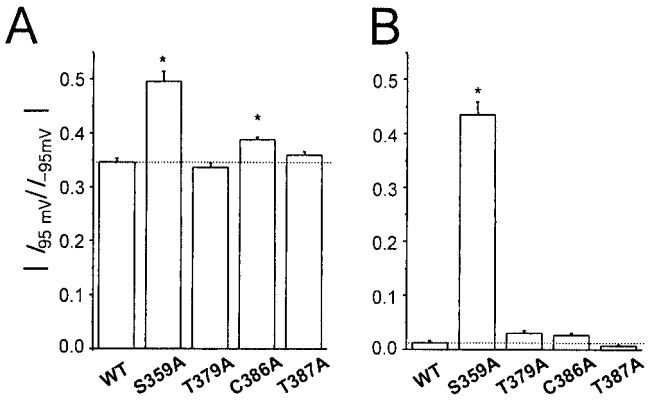

FIGURE 5 Bar graphs represent the degree of current rectifications in wild-type and mutant channels in the presence of 2 μM intracellular Ca^{2+} (*A*) and 2 μM intracellular Ca^{2+} and 10 μM Ba^{2+} (*B*). The ionic currents measured at 95 mV were divided into the currents at -95 mV and the absolute values ($|I_{95mV}/I_{-95mV}|$) were plotted for each channel (*, $p < 0.001$).

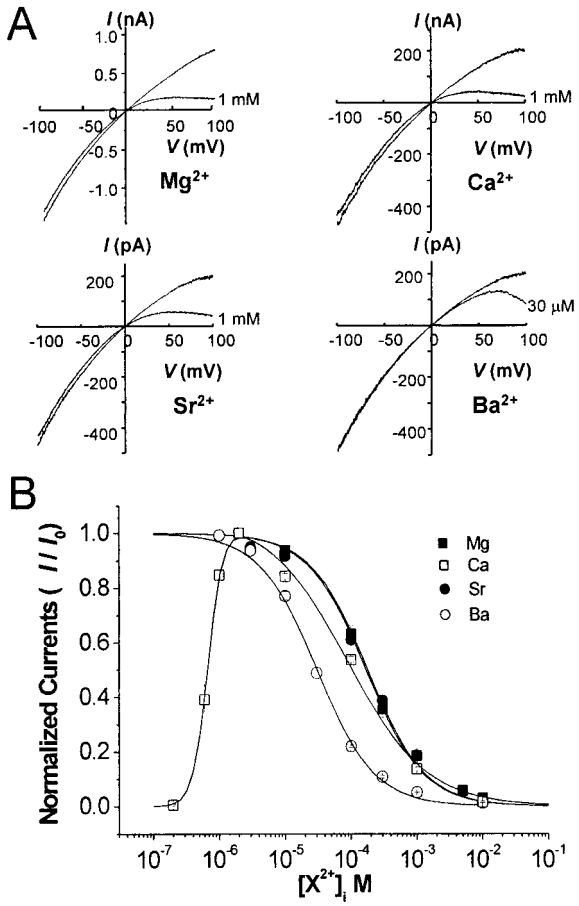

FIGURE 6 Blockade for S359A mutant channel by alkali earth metals. (*A*) Representative traces of S359A control currents activated by 2 μM intracellular Ca^{2+} and the current trace in the presence of indicated concentration of intracellular divalent cation in addition to Ca^{2+} were shown for four different divalent cations, Mg^{2+}, Ca^{2+}, Sr^{2+}, and Ba^{2+}. (*B*) Fraction of unblocked currents (I/I_o) obtained from the normalized currents at 90 mV were plotted against different concentrations of each divalent divalent cation, $[X^{2+}]_i$. The lines superimposed on the data points correspond to least-squares fits using the Hill equation. The observed inhibition constants of each divalent cation were shown in Table 1.

Ala mutation on the affinities of divalent cations varied among different ions. Whereas the apparent affinities of both Ba^{2+} and Sr^{2+} decreased dramatically (51-fold and 46.5-fold, respectively), the affinity for Ca^{2+} decreased only ~4.5-fold (Fig. 6 *B* and Table 1). Moreover, no significant change in Mg^{2+} affinity was detected at 90 mV. Thus, we measured the apparent affinities of these ions at various transmembrane voltages (Fig. 7). The effects of mutation on the voltage dependence of blockade were varied among different divalent cations. Although the apparent affinities of Ba^{2+} decreased greatly, the voltage dependences shown in electrical distance (δ) were not altered significantly (0.45 for wild type and 0.44 for S359A). The voltage dependences of Sr^{2+} and Mg^{2+} for S359A mutant channel were significantly lower, 0.25 and 0.31, respectively. The electrical distance obtained in this experiment cannot be simply interpreted as the relative location of the binding site for each ion, however, because the apparent affinity and the voltage-dependence of intracellular Mg^{2+} blockade for the rSK2 channel is at least in part due to the coupling between Mg^{2+} and K^+ (Soh and Park, 2001). It is also noteworthy that the binding affinity of Mg^{2+} for S359A channel slightly increased at lower positive voltages (see Discussion).

To confirm the direct interaction between amino acid residues of interests within the channel pore and divalent cations, we applied a systematic analysis of a "thermodynamic mutant cycle" (Schreiber and Fersht, 1995; Hidalgo and MacKinnon, 1995). This technique has been applied to identify the pairwise interaction between two proteins or a protein and a peptide, and to quantify the influence of one mutation on the effect of a second mutation as a pairwise coupling energy between two mutated sites (Goldstein et al., 1994; Schreiber and Fersht, 1995; Hidalgo and MacKinnon, 1995; Ranganathan et al. 1996; Zhou et al., 2001b). Because the application of divalent cations of different size to a specific mutant channel is analogous to "double mutation" (Fig. 8 *A*), we should be able to assess the energetic coupling between the ions and the specific residues of the channel. Thus, a coupling coefficient, Ω, for the magnitude of interaction between any perturbation, e.g., mutation and ion switching in this case, is given by:

$$\Omega = \frac{K_D(\mathrm{WT}, A^{2+}) \times K_D(\mathrm{Mut}, \mathrm{B}^{2+})}{K_D(\mathrm{WT}, \mathrm{B}^{2+}) \times K_D(\mathrm{Mut}, \mathrm{A}^{2+})}$$

in which $K_D(X, Y^{2+})$ is the equilibrium constant for channel X and divalent cation Y. Based on the unmutated channel and Mg^{2+} as the wild type, Ω values were obtained from pairwise interaction between five mutant channels and three

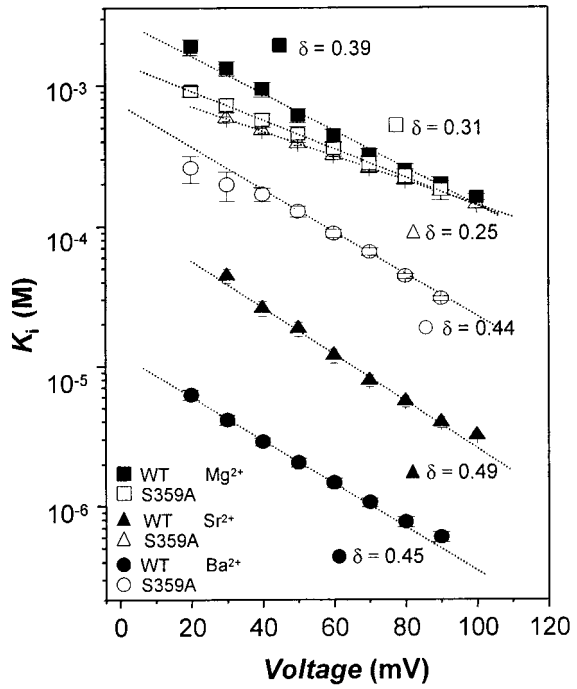

FIGURE 7 Voltage-dependence of divalent blockade for wild-type and S359A mutant channels. The inhibition constants, K_i, of three divalent cations, Mg^{2+}, Sr^{2+}, and Ba^{2+} were plotted against various membrane voltages. The lines superimposed on data points correspond to least-squares fits using the Woodhull (1973) equation, $\ln {}^{X}K_i = \ln {}^{X}K_i\,(0\text{ mV}) - (z\delta)_{obs}FV/RT$, in which ${}^{X}K_i$ and ${}^{X}K_i$ (0 mV) represent the inhibition constants of divalent cation, X, measured at test voltage and 0 mV, respectively. F, R, and T have their usual thermodynamic meaning.

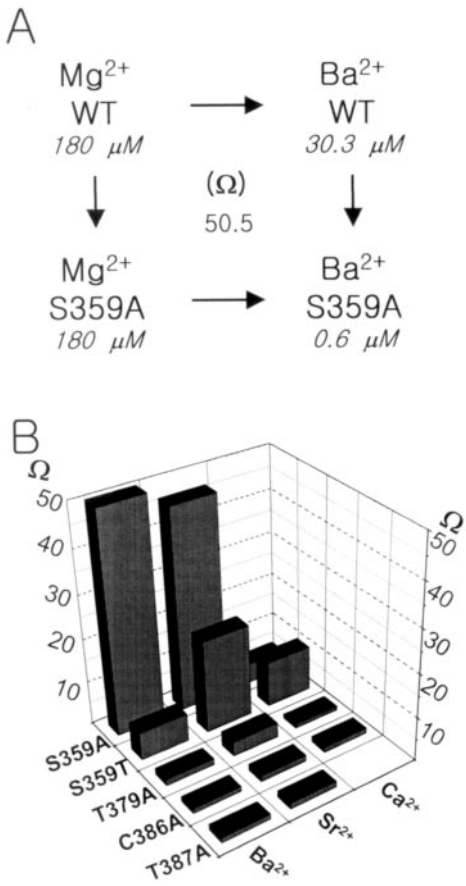

FIGURE 8 Mutant cycle analysis between amino acid residues lining the conduction pore and intracellular divalents. (*A*) Representative mutant cycle showing the interaction between a residue in the P-region, Ser-359, and a divalent cation, Ba^{2+}. The current blockade by intracellular Mg^{2+} and Ba^{2+} were measured for wild-type (WT) and S359A mutant channels in a pair-wise manner, and the inhibition constant (K_i) were shown in italics. A coupling coefficient, Ω, was calculated using an equation, $\Omega = \{K_i(\text{WT}, Mg^{2+}) \times K_i(\text{S359A}, Ba^{2+})\}/\{K_i(\text{WT}, Ba^{2+}) \times K_i(\text{S359A}, Mg^{2+})\}$. When Ser residue was replaced for Ala at the position and the intracellular Mg^{2+} was substituted for Ba^{2+}, a strong energetic coupling, $\Omega = 50.5$, was observed. (*B*) Ω map of amino acid residues in rSK2 channel and intracellular alkali earth metals. The inhibition constants (K_i) of three divalent cations (Ca^{2+}, Sr^{2+}, and Ba^{2+}) on mutant channels of four different positions were obtained in pair-wise manners. Ω of each channel:ion pair was calculated from four K_i values in the mutant cycle, and plotted as bars in the graph. The K_i value of Mg^{2+} on wild-type channel, 180 μM, was used arbitrarily as the control. Ω of T387:Ca^{2+} was not determined.

"mutant" ions. If an ion binds independent of the mutated residue, then Ω will be unity. However, if a divalent cation interacts with the mutated residue and the mutation (or the switching of ion to another one) alters the interaction between them, then Ω will deviate from unity (Zhou et al., 2001b). Among the Ala substitution mutants, large Ω values were detected for Ser-359 when tested with different divalent cations (Fig. 8 *B*, the row of S359A). The pairs of Ser-359-Ala-Ba^{2+} and Ser-359-Ala-Sr^{2+} represent Ω values of 50.5 and 46.5, respectively, and these values correspond to coupling energy, ln Ω of 3.9 and 3.8 kT. However, the Ω values of near unity (1.1 ~ 1.4) were detected for C386 and T387 (Fig. 8 *B*, the rows of C386A and T387A). It is intriguing to find the lack of energetic coupling between C386 and different divalent cations, although the I-V relationship of C386A in the presence of 2 μM intracellular Ca^{2+} is somewhat linear compared with that of wild type as described previously. It is also worth noticing that the small but significant Ω values were detected for T379, and the size of Ω gets progressively smaller for larger ions, 4.6 for Ca^{2+}, 3.3 for Sr^{2+}, and 1.5 for Ba^{2+} (the row of T379A, also see Discussion). Therefore, Ser-359 in the P-region interacts with divalent cation and renders a strong rectification to the I-V relationship of rSK2 channels.

Hydroxyl group is critical for high affinity binding of divalent cations to rSK2

To further investigate the importance of the side chain hydroxyl group of Ser-359 residue in determining the permeation characteristics of the rSK2 channel, we replaced this residue with other amino acids and determined the ion selectivity. Among nine different amino acids (Val, Pro, Lys, Trp, Glu, Ala, Thr, Asn, and Cys) tested, mutant channels with only four amino acids residues, Ala, Thr,

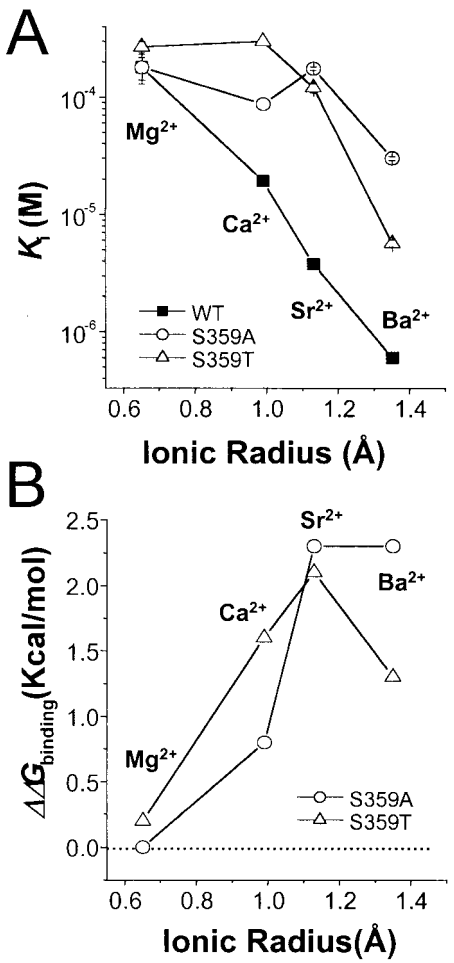

FIGURE 9 Size-selectivity among divalent cations for wild-type, S359T, and S359A mutant channels. (*A*) The inhibition constants (K_i) of different divalent cation for wild type, S359T, and S359A mutant were plotted against ionic radius of each divalent cation. (*B*) The differences in free energy of binding ($\Delta\Delta G$) to the wild type versus S359 mutant channels (S359A and S359T) were plotted against ionic radius. $\Delta\Delta G$ was calculated from an equation, $\Delta\Delta G = RT \ln K_i(\text{mutant})/K_i(\text{WT})$, and the dotted line indicates the level where $\Delta\Delta G = 0$.

Asn, and Cys, expressed measurable currents activated by intracellular calcium. In fact, S359T was the only additional mutant channel other than S359A expressing enough ionic currents for subsequent functional studies. The Ω analysis of S359T also resulted in significantly large Ω values for different divalent cations such as the Ω value of 21.3 (or the coupling energy of 3.1 kT) for Sr^{2+} (Fig. 8 *B*, the row of S359T). The intolerance for mutation at position 359 of the rSK2 channels and the strong conservation of a Ser or Thr residue at the corresponding position among different families of K^+ channels (Fig. 2 *A*) further suggest the importance of hydroxyl groups at this position in permeation of potassium channels in general.

We compared the ion selectivity of wild-type channels and two mutant channels, S359A and S359T, for divalent cations, Mg^{2+}, Ca^{2+}, Sr^{2+}, and Ba^{2+} (Fig. 9 *A* and Table 1). The wild-type channel binds Ba^{2+} with approximately a 300-fold-higher affinity than Mg^{2+}. However, S359A mutant channel is virtually indiscriminative among Mg^{2+}, Ca^{2+}, and Sr^{2+}, and binds Ba^{2+} only about sixfold better than Mg^{2+}. The effects were much smaller for the mutant channel (S359T) containing Ser instead of Thr at this position. Although the affinities for Mg^{2+} and Ca^{2+} were about the same, S359A showed approximately a 50-fold higher affinity for Ba^{2+} compared with Mg^{2+}. In Fig. 8 *B*, the differences in free energy of binding ($\Delta\Delta G_{binding}$) to the wild-type versus the mutant channels were plotted as a function of ionic radius. The apparent affinities of divalent cations to wild type, S359A, and S359T channel are decreased as the size of ion increases. The effects of mutation at Ser-359 are significantly different, however, and the loss of binding energy is highly dependent on the ionic size: the removal of hydroxyl group affects the affinity of larger ions, whereas the addition of one methyl group to β-carbon reduces the binding affinity of Sr^{2+} more selectively. The size selective effects of the mutation at position 359 further support the idea that Ser-359 residue within in the conduction pore directly interacts with the intracellular divalent cations.

DISCUSSION

In the present study, we investigated the effects of Ala mutation on hydrophilic residues likely located within the K^+-conduction pathway of a small conductance Ca^{2+}-activated K^+ channel, rSK2, and tried to localize the divalent cation-binding site affecting the channel's I-V relationship proposed in the previous study (Soh and Park, 2001). We identified a Ser residue, S359, within the P-region of rSK2 making I-V rectification more linear and rendering lower affinities for intracellular divalent cations upon alanine substitution. Although we initially noticed that several aspects of the inward rectification found in SK_{Ca} channels are similar with that of K_{ir} channels, the mechanism of action turns out to be different between these two types of potassium channels at the molecular level. While the intracellular cations interact with a charged (or hydrophilic) residue presumably located in the "central cavity" of K_{ir} channels, divalent cations bind to Ser residues near the K^+-selectivity filter of SK_{Ca} channels.

The location of divalent cation-binding site is presumed to be near the K^+-selectivity filter of rSK_{Ca} channel based on the alignment of amino acid sequence (Fig. 2 *B*) and the known structure of a bacterial K^+ channel, KcsA (Doyle et al., 1998). The site coordinated by the Ser-359 residue of rSK2 is likely to co-localize with the "Ba^{2+} site" near Thr-75 of the KcsA channel (Fig. 2 *B*, highlighted in red). The electron density of Ba^{2+} in the KcsA channel was revealed to superimpose with the electron density of Rb^+, the one closer to the pore cavity of the two densities, at the

"inner ion" site of K^+-selectivity filter (Jiang and MacKinnon, 2000). More recently, the resolution of the KcsA channel structure was further improved and the electron densities of K^+ ions were revealed at seven different positions in the conduction pathway including four K^+-binding sites within the selectivity filter (Zhou et al., 2001a). This recent structure showed that the hydroxyl group of Thr-75 directly coordinates the K^+ ion at the fourth position of the selectivity filter closer to the central cavity. Thus, the divalent cation-binding site created by Ser-359 in SK_{Ca} channels may also be involved in the selective binding of K^+ during ion permeation. It is intriguing to find that SK_{Ca} channels are the only subfamily containing Ser residues in this position, e.g., Ser-359 of rSK2, among the various K^+ channels. All other subfamilies of K^+ channels including the most homologous IK_{Ca} channels have Thr residues instead of Ser at the corresponding positions. Therefore, it remains to be investigated whether the Ser residue plays important roles in determining other pore properties of SK_{Ca} channel such as selectivity for monovalent cations and single-channel conductance.

We were able to detect strong energetic couplings between Ser-359 and different divalent cations tested using a modified version of thermodynamic mutant cycles (Fig. 8), further supporting the direct interaction between the residue and ions. Small but significant couplings were detected between another residue, Thr-379, and divalent cations. Moreover, the coupling coefficients were progressively smaller as the size of divalent cations was increased from 4.6 to 1.5. This is intriguing since the corresponding residue in the KcsA channel, Val-95, does not participate in the lining of the conduction pore but is located at the extracellular side of the "inner helix" involved in the surface interaction with the "pore-helix" (Doyle et al., 1998). Thus, the small coupling energy ($\ln \Omega$) of 1.5 kT (or Ω of 4.6) found at Thr-379 can be considered indirect effects (Ranganathan et al., 1996) and may be due to the local structural changes sensed by the divalent cation-binding site via the "pore-helix" of rSK2 channel.

The hydroxyl group at position 359 seems to be critical for high affinity binding and selectivity of divalent cations for the site, indicating that the residue directly interacting with different divalent cations. It is particularly interesting that this site interacts with divalent cations with relatively high affinity, e.g., ${}^{Ca}K_i$ of $\sim$20 μM and ${}^{Ba}K_i$ of $\sim$0.6 μM (Table 1) without any carboxyl group involved. This high affinity for divalent cations may be contributed by the optimal arrangement of hydroxyl groups within the narrow pore of the channel, since even the conserved mutation of Ser to Thr significantly alters the selectivity of the site for a larger ion, Ba^{2+} (Fig. 9). Ser-359 residue is not the sole determinant of the strongly rectified I-V relationship of SK_{Ca} channels, because the I-V relationship of S359A mutant channel still bears a significant inward rectification (Figs. 4 *A* and 5 *A*). The remaining inward rectification of the mutant channel is not due to the residual affinity for Ca^{2+} after the Ala substitution, however, because the blockade of channel currents is only minimal in the presence of the marginal concentration of 2 μM Ca^{2+} (Fig. 6 *B*). It is also worth pointing out that the homotetrameric S359A channel still showed a respectable affinity for Ba^{2+} (${}^{Ba}K_i$ = 30 μM) even with the absence of four hydroxyl groups. Thus, it needs to be determined whether carbonyl oxygens or side-chains of adjacent amino acid residues contribute to the site for coordinating divalent cations. It is interesting to find that the K^+ ion at the corresponding site (position 4) of the KcsA selectivity filter is coordinated by not only the backbone carbonyl oxygens but also the hydroxyl groups of Thr-75 residues from four different subunits (Zhou et al., 2001a).

We noticed that the affinity of Mg^{2+} for S359A mutant channel was not changed at 90 mV and was even slightly but significantly increased at lower positive voltages (Fig. 7). It is still unclear what caused this seemingly contradictory result and there could be several different possibilities. One of such possibilities is that this may be the manifestation of altered interaction between Mg^{2+} and K^+ within the conduction pore upon mutation. In our previous study (Soh and Park, 2001) we showed that the permeant ions and intracellular blocking ions interact within the conduction pore of rSK2 channel and that this interaction affects both the apparent affinity and the voltage-dependence of divalent cation blockade. The Ser to Ala mutation at 359 could alter the interaction between Mg^{2+} and K^+ as well as the intrinsic affinity of Mg^{2+} to the site. It remains to be investigated experimentally whether such a mechanism can explain the unique behavior of Mg^{2+} on S359A mutant channel.

The selectivity for divalent cations of the blocking site, $Ba^{2+} > Sr^{2+} > Ca^{2+} > Mg^{2+} >$ (Fig. 9 *A*), is in the reverse order of SK_{Ca} channel activation, $Ca^{2+} > Sr^{2+} > Ba^{2+}$ (Soh and Park, 2001), determined by calmodulin. Although intracellular Mg^{2+} failed to activate rSK2 currents even at 20 mM (Soh and Park, 2001), the affinity of Mg^{2+} revealed in this study, ${}^{Mg}K_i$ of 180 μM for rSK2, indicates that a significant portion of outward currents should be blocked by physiological concentrations of Mg^{2+}. SK_{Ca} channels are activated at submicromolar range of intracellular Ca^{2+} in a highly cooperative manner, ${}^{Ca}K_{1/2}$ of 0.55 μM and *n* of 4 .1 for rSK2 (Soh and Park, 2001), and the channel currents are blocked by two orders of magnitude lower range of Ca^{2+} concentration, ${}^{Ca}K_i$ of 19.3 μM. Because the local concentration of intracellular Ca^{2+} in neurons is known to increase up to tens of micromolar after the firing of action potentials (Regehr and Tank, 1992), the permeation of K^+ ions through SK_{Ca} channels can be affected by these dynamic changes of intracellular Ca^{2+} as well as the tonic blockade by Mg^{2+}.

In conclusion, we localized a divalent cation-binding site within the conduction pathway of rSK2, and revealed the direct interaction between a serine residue, Ser-359, and

divalent cations. We also confirmed that the binding of divalent cation at this site and thus the blockade of K^+ conduction by the binding contribute the inwardly rectified I-V relationship of the SK_{Ca} channel.

The authors wish to thank Dr. John P. Adelman (The Vollum Institute, Oregon Health Sciences University) for providing rSK2 cDNA. We also thank Dr. C. Miller for his valuable comments, J. Lee for reading the manuscript, and the other members of Molecular Neurobiology Laboratory at K-JIST for their help throughout this work. This research was supported by the Ministry of Science and Technology of Korea, Critical Technology 21-Life Phenomena and Function Research Grant 01-J-LF-01-B-54, Brain Neurobiology Research Grant M1–0108-00-005, and the Korea Research Foundation Grant BK21 (to C.-S. Park).

REFERENCES

Bond, C. T., M. Pessia, X. M. Xia, A. Lagrutta, M. P. Kavanaugh, and J. P. Adelman. 1994. Cloning and expression of a family of inward rectifier potassium channels. *Recept. Channels.* 2:183–191.

Doyle, D. A., J. Morais Cabral, R. A. Pfuetzner, A. Kuo,. J. M. Gulbis, S. L. Cohen, B. T. Chait, and R. MacKinnon. 1998. The structure of the potassium channel: molecular basis of K^+ conduction and selectivity. *Science.* 280:69–77.

Goldstein, S. A., D. J. Pheasant, and C. Miller. 1994. The charybdotoxin receptor of a Shaker K^+ channel: peptide and channel residues mediating molecular recognition. *Neuron.* 12:1377–1388.

Hidalgo, P., and R. MacKinnon. 1995. Revealing the architecture of a K^+ channel pore through mutant cycles with a peptide inhibitor. *Science.* 268:307–310.

Hille, B. 1991. Ionic Channels of Excitable Membranes. Sinauer, Sunderland, MA.

Ho, K., C. G. Nichols, W. J. Lederer, J. Lytton, P. M. Vassilev, M. V. Kanazirska, and S. C. Hebert. 1993. Cloning and expression of an inwardly rectifying ATP-regulated potassium channel. *Nature.* 362: 31–38.

Jiang, Y., and R. MacKinnon. 2000. The barium site in a potassium channel by x-ray crystallography. *J. Gen. Physiol.* 115:269–272.

Keen, J. E., R. Kawaled, D. L. Farrens, T. Neelands, A. Rivard, C. T. Bond, A. Janowsky, B. Fakler, J. P. Adelman, and J. Maylie. 1999. Domains responsible for constitutive and Ca^{2+}-dependent interactions between calmodulin and small conductance Ca^{2+}-activated potassium channels. *J. Neurosci.* 19:8830–8838.

Kohler, M., B. Hirschberg, C. T. Bond, J. M. Kinzie, N. V. Marrion, J. Maylie, and J. P. Adelman. 1996. Small-conductance, calcium-activated potassium channels form mammalian brain. *Science.* 273:1709–1914.

Kubo, Y., T. J. Baldwin, Y. N. Jan, and L. Y. Jan. 1993. Primary structure and functional expression of a mouse inward rectifier potassium channel. *Nature.* 362:127–133.

LeMasurier, M., L. Heginbotham, and C. Miller. 2001. KcsA: it's a potassium channel. *J. Gen. Physiol.* 118:303–313.

Lopatin, A. N., and C. G. Nichols. 1996. $[K^+]$ dependence of polyamine-induced rectification in inward rectifier potassium channels (IRK, Kir2.1). *J. Gen. Physiol.* 108:105–113.

Lu, Z., A. M. Klem, and Y. Ramu. 2001. Ion conduction pore is conserved among potassium channels. *Nature.* 413:809–813.

Lu, Z., and R. MacKinnon. 1994. Electrostatic tuning of Mg^{2+} affinity in an inward-rectifier K^+ channel. *Nature.* 371:243–245.

Martell, A. E., and R. M. Smith. 1974. Critical Stability Constants. Vol. 1. Plenum, New York.

Matsuda, H., A. Saigusa, and H. Irisawa. 1987. Ohmic conductance through the inward-rectifier K^+ channel and blocking by internal Mg^{2+}. *Nature.* 325:156–159.

Ranganathan, R., J. H. Lewis, and R. MacKinnon. 1996. Spatial localization of the K^+ channel selectivity filter by mutant cycle-based structure analysis. *Neuron.* 16:131–139.

Regehr, W. G., and D. W. Tank. 1992. Calcium concentration dynamics produced by synaptic activation of CA1 hippocampal pyramidal cells. *J. Neurosci.* 12:4202–4223.

Schreiber, G., and A. R. Fersht. 1995. Energetics of protein-protein interactions: analysis of the barnase-barstar interface by single mutations and double mutant cycles. *J. Mol. Biol.* 248:478–486.

Shrivastava, I. H., C. E. Capener, L. R. Forrest, and M. S. Sansom. 2000. Structure and dynamics of K channel pore-lining helices: a comparative simulation study. *Biophys. J.* 78:79–92.

Soh, H., and C.-S. Park. 2001. Inwardly rectifying current-voltage relationship of small-conductance Ca^{2+}-activated K^+ channels rendered by intracellular divalent cation blockade. *Biophys. J.* 80:2207–2215.

Vandenberg, C. A. 1987. Inward rectification of a potassium channel in cardiac ventricular cells depends on internal magnesium ions. *Proc. Natl. Acad. Sci. U. S. A.* 84:2560–2564.

Vergara, C., R. Latorre, N. V. Marrion, and J. P. Adelman. 1998. Calcium-activated potassium channels. *Curr. Opin. Neurobiol.* 8:321–329.

Wible, B. A., M. Taglialatela, E. Ficker, and A. M. Brown. 1994. Gating of inwardly rectifying K^+ channels localized to a single negatively charged residue. *Nature.* 371:246–249.

Williams, K. 1997. Interactions of polyamines with ion channels. *Biochem. J.* 325:289–708.

Woodhull, A. M. 1973. Ionic blockage of sodium channels in nerve. *J. Gen. Physiol.* 61:687–708.

Xia, X. M., B. Fakler, A. Rivard, G. Wayman, T. Johnson-Pais, J. E. Keen, T. Ishii, B. Hirschberg, C. T. Bond, S. Lutsenko, J. Maylie, and J. P. Adelman. 1998. Mechanism of calcium gating in small-conductance calcium-activated potassium channels. *Nature.* 395:503–507.

Zhou, M.,. H. Morais-Cabral, A. Kaufman, and R. MacKinnon. 2001a. Chemistry of ion coordination and hydration revealed by a K^+ channel-Fab complex at 2.0 A resolution. *Nature.* 414:43–48.

Zhou, M., J. H. Morais-Cabral, S. Mann, and R. MacKinnon. 2001b. Potassium channel receptor site for the inactivation gate and quaternary amine inhibitors. *Nature.* 411:657–61.